Received: 29 August 2021 | Revised: 7 April 2022 | Accepted: 30 May 2022

DOI: 10.1111/1440-1681.13683

ORIGINAL ARTICLE

CEPP Clinical and Experimental Pharmacology and Physiology WILEY

Dihydroartemisinin protects blood–brain barrier permeability during sepsis by inhibiting the transcription factor SNAI1

Fuhong Liu[1,2] | Jing Liu[2] | Hongjie Xiang[3] | Zongguo Sun[2] | Yan Li[1] | Xiao Li[1] | Yanjun Liu[1] | Ju Liu[2]

[1]School of Traditional Chinese Medicine, Shandong University of Traditional Chinese Medicine, Jinan, China

[2]Medical Research Center, the First Affiliated Hospital of Shandong First Medical University & Shandong Provincial Qianfoshan Hospital, Jinan, China

[3]Department of Traditional Chinese Medicine, The First Affiliated Hospital of Shandong First Medical University & Shandong Provincial Qianfoshan Hospital, Jinan, China

Correspondence
Ju Liu, Medical Research Center, the First Affiliated Hospital of Shandong First Medical University & Shandong Provincial Qianfoshan Hospital, 16766 Jingshi Road, Jinan, Shandong 250014, China.
Email: ju.liu@sdu.edu.cn

Funding information
This study was supported by the National Nature Science Foundation of China (82171318, 81873473 and 91939110), Academic Promotion Program of Shandong First Medical University (2019QL014), Jinan City's Science and Technology Innovation Program of Clinical Medicine (202019175) and Shandong Taishan Scholarship (J.L.); Cultivation Fund for the First Affiliated Hospital of Shandong First Medical University: QYPY2021NSFC0613

Abstract

Blood–brain barrier (BBB) injury is involved in the pathogenesis of sepsis-associated encephalopathy. In this study, we used dihydroartemisinin (DHA), a derivative of artemisinin, to treat a cecal ligation and puncture (CLP)-induced mouse sepsis model and a tumour necrosis factor α (TNF-α)-stimulated human cerebral microvessel endothelial cells (hCMEC)/D3 cell line. We found that DHA decreased BBB permeability and increased the expression of the tight junction protein occludin (OCLN) in the CLP model. In hCMEC/D3 cells, DHA decreased TNF-α-induced hyperpermeability and increased the expression of OCLN. DHA also repressed SNAI1 expression in the CLP mouse model and in TNF-α-stimulated hCMEC/D3 cells. These data suggest that DHA protects BBB permeability during sepsis by stimulating the expression of OCLN, by downregulating the expression of the SNAI1 transcription factor.

KEYWORDS
blood–brain barrier, dihydroartemisinin, occludin, Qinghao, sepsis, SNAI1

1 | INTRODUCTION

Sepsis is a life-threatening organ dysfunction caused by an infection. It is the most common cause of mortality in intensive care units (ICU), leading to approximately six million deaths annually.[1,2] Sepsis-associated encephalopathy (SAE) is one of the complications of sepsis. Previous studies have reported that up to 70% of septic patients suffered from SAE.[1,3] However, the pathophysiological mechanism of SAE is not fully understood.

Blood–brain barrier (BBB) injury is involved in the pathogenesis of SAE.[4] BBB is a semipermeable border mainly composed of vascular endothelial cells (ECs). It prevents small molecules such as drugs from non-selectively crossing into the central nervous system.[5] ECs are connected to the adjacent cells by a series of junctional complexes, including adherens junction proteins (AJs) and tight junction proteins (TJs). Transmembrane TJs (including occludin [OCLN]) are the main determinants of BBB permeability. They form junctions between

adjacent ECs and anchor to the actin cytoskeleton through cytoskeletal scaffolding proteins.[6] During inflammation conditions, increased BBB permeability is induced by proinflammatory cytokines, endotoxin, mediators, reactive oxygen species (ROS) and nitric oxide (NO).[1,7] As a consequence, the breakdown of the BBB causes damage to the neural tissue.[1,3]

Artemisinin is a sesquiterpene lactone compound; it is the major extract of Qinghao (*Artemisia annua* L.). Artemisinin and its derivatives are safe and efficient anti-malaria drugs.[8] Moreover, artemisinins may affect inflammation, angiogenesis and cancer.[9–11] In sepsis, artemisinins were reported to protect septic mice by inhibiting the release of inflammatory factors and regulating macrophage autophagy.[12,13] However, whether artemisinins could attenuate the noxious effect of inflammation factors in sepsis remains unclear. Previous studies reported that artemisinins could protect BBB breakdown in a cerebral malaria mouse model and in a subarachnoid haemorrhage rat model.[14,15] Therefore, we predict that artemisins might protect the BBB from sepsis.

OCLN is a tetraspanin protein containing two extracellular loops, an intracellular loop and cytosolic N and C termini. The C-terminal domain of OCLN binds to ZO-1 and ZO-2 in the cytoplasm.[16–18] OCLN contributes to the formation of the TJ network and to BBB function.[19] A recent clinical study revealed no or low OCLN expression (in human autopsy specimens) in 38% (18/47) of the patients with sepsis reaching the cerebral microvessel endothelium.[20] This suggested that OCLN reduction might be involved in sepsis pathophysiological process.

Snail family transcriptional repressor 1 (SNAI1) is a member of the Snail family of transcriptional repressors. Its C-terminal highly conserved region contains four C_2H_2 type zinc finger domains.[21] These domains specifically recognized the target sequence also known as the E-box motif (containing the core sequence CAGGTG).[21,22] SNAI1 is involved in normal embryogenesis processes, organ fibrosis and tumour metastasis.[23–25] Furthermore, studies have suggested that SNAI1 participates in regulating BBB permeability.[26,27] It can directly bind to E-boxes of several TJ genes, such as *OCLN* and *claudins*, blocking their promoters and therefore, inhibiting their transcription and affecting intercellular permeability.[27]

In the present study, we investigated the effects of dihydroartemisinin (DHA) (an active metabolite of artemisinins) in the cecal ligation and puncture (CLP) mouse model and tumour necrosis factor α (TNF-α)-stimulated human cerebral microvascular endothelial cell (hCMEC/D3).

2 | RESULTS

2.1 | DHA prevents increased permeability of the BBB in a CLP mouse model

Previous studies suggested that BBB permeability increases in the CLP model.[28,29] To test the effect of DHA on the permeability of BBB in septic mice, we administrated DHA to CLP model mice by gavage (100 mg/kg/day). As shown in Figure 1A, mice in the CLP group exhibited decreased BBB integrity than mice from the sham group. In contrast, DHA administration reduced BBB permeability in the CLP + DHA group compared to that in the CLP group ($P < .01$). Subsequently, a brain water content assay was performed as an additional permeability index. As shown in Figure 1B, mice in the CLP group exhibited a significant increase in brain water content, and DHA administration caused a dramatic decrease in brain water content in the CLP + DHA group compared with that in the CLP group ($P < .01$).

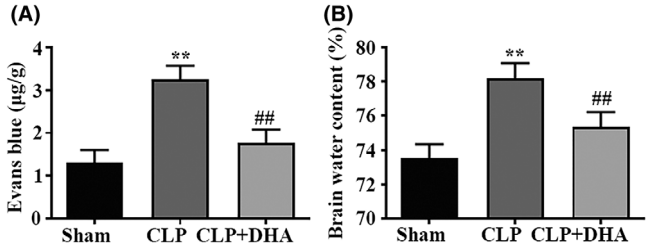

FIGURE 1 DHA prevents increased permeability of BBB in a CLP mouse model. A, Evans blue dye extravasation was measured to examine the integrity of BBB. B, Brain water content was measured by the dry-wet method. n = 6. $^{**}P < .01$ vs the sham group, $\#\#P < .01$ vs the CLP group. DHA, dihydroartemisinin; BBB, blood–brain barrier; CLP, cecal ligation and puncture

Additionally, at 24 h post operation, the effect of DHA on TNF-α levels in the serum and brain tissue of CLP mice was examined (-Figure S1). The levels of TNF-α in the serum and brain tissue were significantly increased in the CLP group compared with that in the sham group. In the CLP + DHA group, the levels of TNF-α were significantly lower than those in the CLP group ($P < .01$).

2.2 | DHA attenuates the decrease in OCLN levels observed in the CLP mouse model

BBB permeability is mainly determined by the TJs between two brain endothelial cells (BECs); The surface edges are effectively sealed by junctional molecules that limit penetration across BECs.[6] We isolated brain microvessel endothelial cells to examine the expression of OCLN. Real-time quantitative polymerase chain reaction (RT-qPCR) analysis showed a significant 49% decrease in *Ocln* messenger RNA (mRNA) expression in the CLP group compared to that in the sham group. In addition, *Ocln* mRNA expression increased significantly, by 20.5% in the CLP + DHA group compared to that in the CLP group (Figure 2A). Western blotting showed that the same tendency (Figure 2B). Moreover, immunohistochemistry (IHC) and immunofluorescence (IF) assays showed that OCLN was specifically expressed in mouse BECs, and the expression levels were significantly decreased in the CLP group compared to those in the sham group and CLP + DHA groups. However, there was no significant difference in OCLN levels between the sham and CLP + DHA groups (Figure 2C,D). These results showed that DHA increased OCLN expression in mice from the CLP group.

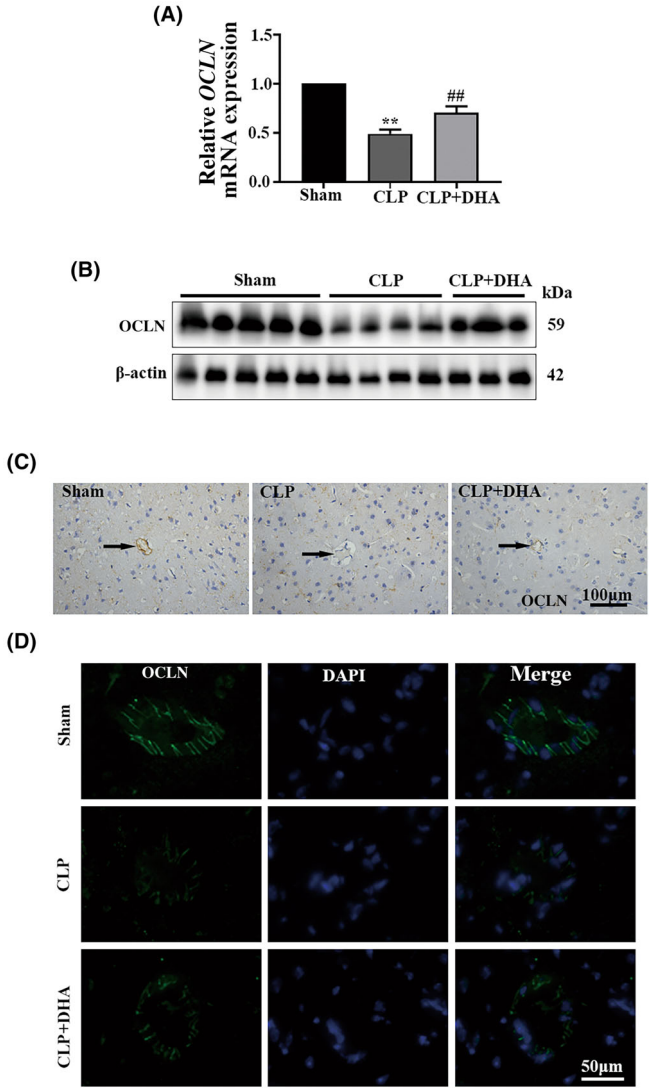

FIGURE 2 DHA protected BBB permeability in CLP mouse models by increasing OCLN content. A, RT-qPCR analyses of relative *Ocln* mRNA levels in brain microvascular endothelial cells of experimental mice. n = 3. $^{**}P < .01$ vs the sham group, $\#\#P < .01$ vs the CLP group. B, OCLN and β-actin protein content in mice brain microvessels evaluated by western blotting. C, IHC on brain endothelial cells for determining OCLN expression. Scale bar: 100 μm. E, IF staining for OCLN detection in brain tissues of experimental mice. Cell nuclei were stained with DAPI (blue). Scale bar: 50 μm. DHA, dihydroartemisinin; BBB, blood–brain barrier; CLP, cecal ligation and puncture; OCLN, occludin; RT-qPCR, real-time quantitative polymerase chain reaction; mRNA, messenger RNA; IHC, immunohistochemistry; IF, immunofluorescence; DAPI, 4',6-diamidino-2-phenylindole

2.3 | DHA reverses TNF-α-induced hyperpermeability of hCMEC/D3 cells

A previous study showed that TNF-α (10 ng/mL) could significantly decrease the expression of OCLN in hCMEC/D3 cells.[30] OCLN is one of the major TJs; its deficiency increases the permeability of BBB.[16] To determine whether DHA inhibits OCLN expression in TNF-α-stimulated hCMEC/D3 cells, we pretreated hCMEC/D3 cells with

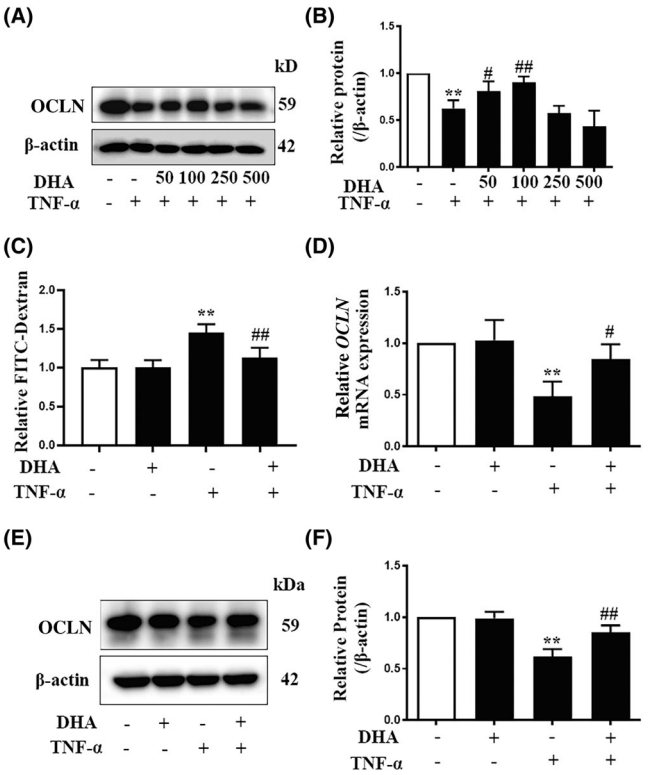

FIGURE 3 DHA reduces hyperpermeability in TNF-α-treated hCMEC/D3 cells. A, Representative immunoblots of OCLN in hCMEC/D3 cells treated with TNF-α and different concentrations of DHA. β-actin was used as the internal control. B, Densitometry analysis of OCLN/β-actin. C, Permeability of hCMEC/D3 monolayers was evaluated by a FITC-dextran transwell assay. Cells were treated with TNF-α and/or DHA. D, Relative mRNA expression of *OCLN* in hCMEC/D3 cells treated with TNF-α and/or DHA. β-actin was used as the internal control. E, Western blot analysis showing OCLN contents in hCMEC/D3 cells treated with TNF-α and/or DHA. β-actin was used as the loading control. F, Protein band densitometric analysis to determine changes in the expression of OCLN in cells from different treatments. n = 3. $^{**}P < .01$ vs the control group, $\#P < .05$ vs the TNF-α group, $\#\#P < .05$ vs the TNF-α group. DHA, dihydroartemisinin; TNF-α, tumour necrosis factor α; hCMEC, human cerebral microvessel endothelial cells; OCLN, occludin; FITC, fluorescein isothiocyanate; mRNA, messenger RNA

different concentrations of DHA for 1 h, and then treated the cells with TNF-α (10 ng/mL) for 24 h. We found that 50 ng/mL ($P < .05$) and 100 ng/mL ($P < .01$) DHA increased OCLN expression significantly. In contrast, TNF-α concentrations of 250 and 500 ng/mL DHA decreased TNF-α-modulated OCLN expression (Figure 3A,B). Cell viability was measured after DHA and/or TNF-α treatments. The results showed that 250 and 500 ng/mL DHA inhibited the viability of hCMEC/D3 cells significantly ($P < .05$) (Figure S2). A total of 100 ng/mL DHA pretreatment for 1 h was used in follow-up experiments to explore the mechanisms of DHA against TNF-α-induced OCLN expression. The permeability of hCMEC/D3 cells was further examined by measuring fluorescein isothiocyanate (FITC)-dextran

concentration after a transwell assay. As was shown in Figure 3C, we found that TNF-α increased the permeability of hCMEC/D3 cells compared with the control group, whereas DHA attenuated this effect. Importantly, DHA alone did not affect the permeability of hCMEC/D3 cells. We performed RT-qPCR to examine the *OCLN* expression and found that treating cells with DHA (1 h) pretreatment significantly increased *OCLN* mRNA levels in TNF-α-treated hCMEC/D3 cells ($P < .01$) (Figure 3C). Additionally, we performed Western blotting to evaluate the protein expression of OCLN protein; the result was similar to that of observed for *OCLN* mRNA (Figure 3D,E). Importantly, DHA alone did not affect OCLN expression (neither at mRNA nor at protein levels) in TNF-α hCMEC/D3 cells (Figure 3C-F). These findings indicate that DHA reduces TNF-α-induced hyperpermeability in hCMEC/D3 cells and might related to OCLN reduction.

2.4 | DHA reduces SNAI1 expression in CLP mouse models and TNF-α-induced hCMEC/D3 cells

It has been reported that SNAI1 contributes to the regulation of the permeability of BECs.[26] Therefore, we investigated whether SNAI1 was involved in the effect of DHA against hyperpermeability in CLP or TNF-α-stimulated BECs. As shown in Figure 4A, *Snai1* mRNA expression significantly increased in the microvessels of the CLP group compared to those of the sham group, whereas DHA inhibited this effect. Consistently, DHA also reversed SNAI1 protein expression in the CLP group (Figure 4B,C). We then examined the effects of DHA on SNAI1 expression of TNF-α-treated hCMEC/D3 cells. As shown in Figure 4D, TNF-α induced the expression of *SNAI1* in hCMEC/D3 cells. Moreover, these effects were inhibited by DHA. We performed Western blotting to evaluate the expression of SNAI1 at the protein level. Our results showed that DHA reversed the increased expression of SNAI1 in hCMEC/D3 cells (Figure 4E,F). The IF results showed the same tendency (Figure 4G). However, DHA alone had no significant effect on SNAI1 expression at either the mRNA or protein levels (Figure 4D-G). These results demonstrate that DHA may decrease the expression of SNAI1 in an in vivo CLP model and in in vitro TNF-α-treated hCMEC/D3 cells.

2.5 | DHA reverses reduced OCLN expression mediated by SNAI1 in TNF-α-treated hCMEC/D3 cells

It has been reported that SNAI1 could transcriptionally repress the expression of OCLN.[27] Therefore, we treated experimental cells with a small interfering RNA (siRNA) (si-SNAI1) against OCLN and performed RT-qPCR and western blotting to measure OCLN expression (Figure 5A). Si-SNAI1 significantly upregulated *OCLN* mRNA levels in hCMEC/D3 cells compared to that of negative control (NC)-siRNA group ($P < .01$). As shown in Figure 5B, si-SNAI1 significantly increased OCLN protein levels as well. SNAI1 overexpression (using a pCMV6-*SNAI1* vector) in hCMEC/D3 cells to test its role in TNF-α-treated cells. pCMV6-Entry vector was used as the control. We

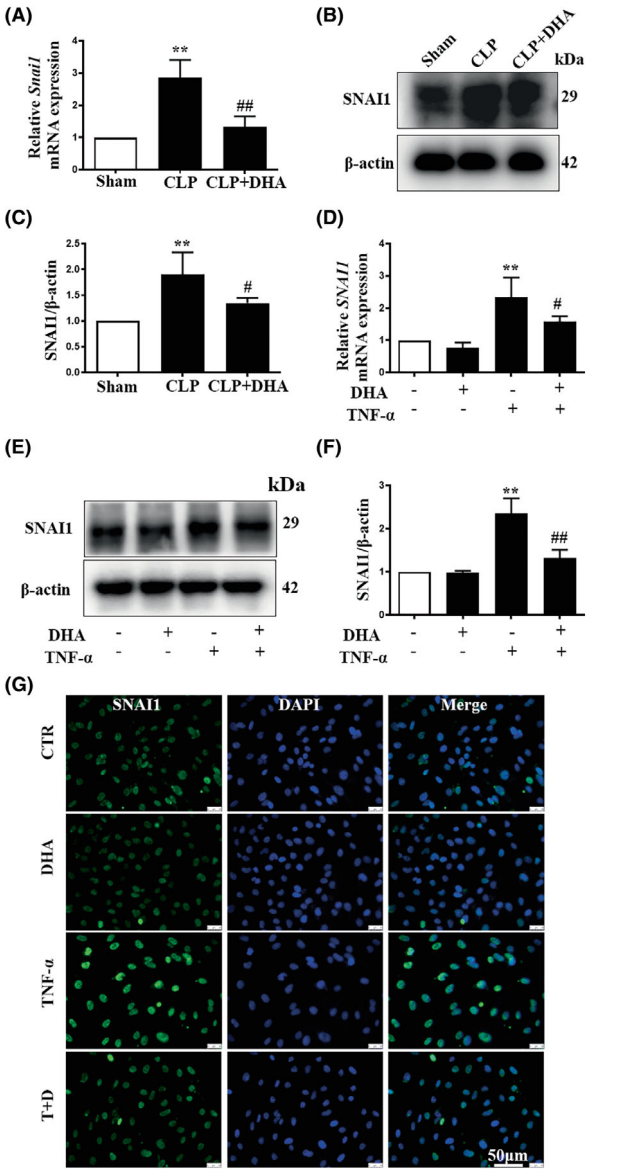

FIGURE 4 DHA reversed SNAI1 expression in CLP mouse models and TNF-α-treated hCMEC/D3 cells. A, Relative *Snai1* mRNA expression in mice brain tissue microvessels. β-actin was used as the internal control. n = 3. $^{**}P < .01$ vs the sham group, $\#\#P < .01$ vs the CLP group. B, Representative immunoblots for the detection of the SNAI1 protein produced in mice brains in the presence and absence of DHA. C, Densitometry analysis of SNAI1/β-actin, the results are expressed as means ± SD. n = 3. $^{**}P < .01$ vs the sham group, $\#P < .05$ vs the CLP group. D, Relative mRNA expression of *SNAI1*, determined by RT-qPCR, in hCMEC/D3 cells treated with TNF-α and/or DHA. β-actin was used as the internal control. n = 3. $^{**}P < .01$ vs the control group, $\#P < .05$ vs the TNF-α group. E, Representative immunoblots of SNAI1 protein in TNF-α and/or DHA-treated hCMEC/D3 cells. F, Densitometry analysis of SNAI1/β-actin, the results are expressed as mean ± SD. n = 3. $^{**}P < .01$ vs the control group, $\#P < .01$ vs the TNF-α group. G, Representative IF staining images of SNAI1 in hCMEC/D3 cells. Cell nuclei were stained with DAPI (blue). DHA, dihydroartemisinin; SNAI1, snail family transcriptional repressor 1; CLP, cecal ligation and puncture; TNF-α, tumour necrosis factor α; hCMEC, human cerebral microvessel endothelial cells; mRNA, messenger RNA; SD, standard deviation; RT-qPCR, real-time quantitative polymerase chain reaction; IF, immunofluorescence; DAPI, 4',6-diamidino-2-phenylindole

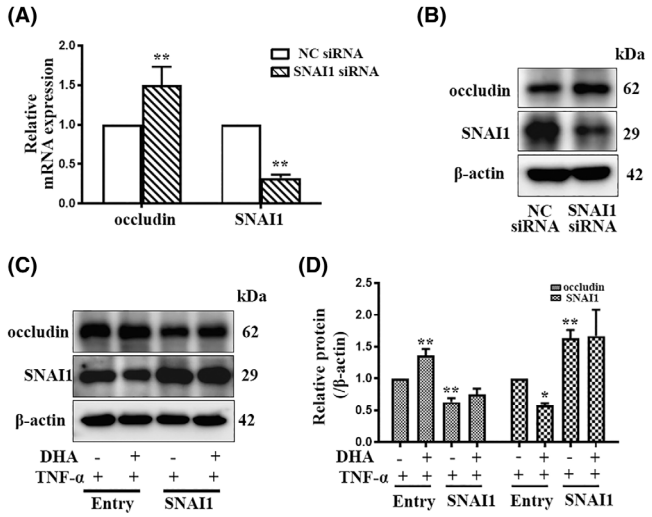

FIGURE 5 DHA reversed OCLN expression in TNF-α-treated hCMEC/D3 cells through SNAI1. A, mRNA expression of *OCLN* and *SNAI1* in hCMEC/D3 cells treated with a siRNA against SNAI1. β-actin was used as the internal control. n = 3. $^{**}P < .01$ vs the NC siRNA group. B, Protein expression of OCLN and SNAI1 in hCMEC/D3 cells treated with siRNA against SNAI1. C, Representative immunoblots showing the expression of OCLN and SNAI1 in hCMEC/D3 cells treated with the pCMV6-*SNAI1* vector in the presence of TNF-α, with or without DHA. D, Relative concentrations of OCLN and SNAI1 proteins in relation to β-actin abundance, determined by densitometric analysis. n = 3. $^{*}P < .05$ vs the TNF-α Entry vector group, $^{**}P < .01$ vs the TNF-α Entry vector group. DHA, dihydroartemisinin; OCLN, occludin; TNF-α, tumour necrosis factor α; hCMEC, human cerebral microvessel endothelial cells; mRNA, messenger RNA; siRNA; small interfering; NC, negative control

observed that overexpression not only caused a significant increase ($P < .01$) in SNAI1, but also a significant decrease in OCLN levels in TNF-α-treated hCMEC/D3 cells ($P < .01$). However, DHA did not reverse this effect ($P > .05$) (Figure 5C,D). These data suggest that DHA regulates OCLN expression in TNF-α-treated hCMEC/D3 cells mediated via SNAI1.

3 | DISCUSSION

In the present study, DHA administration reduced BBB permeability in the CLP sepsis mice model. DHA also reduced TNF-α-induced hyperpermeability of hCMEC/D3 cells TNF-α. Moreover, we found that SNAI1 downregulation was involved in the protective effect of DHA on BBB permeability as it resulted in the upregulation of OCLN expression.

Artemisinins are safe and effective for treating inflammation, angiogenesis and cancer, with few side effects.[31–34] The effect of artemisinins has also been investigated in neuroinflammation-related central nervous system diseases.[34,35] They work by inhibiting systemic inflammatory factors and maintaining BBB integrity in vivo.[34] We also found that DHA inhibited the TNF-α levels of CLP mice serum and brain. There was little research on the protective effect on artemisinins in sepsis BBB permeability. Here, we found that DHA reduced BBB permeability using Evans blue dye and brain water content assay. However, the precise mechanism of BBB protection under inflammatory conditions remains unclear. During sepsis, increased levels of inflammatory cytokines, especially TNF-α, binds to their receptors and induce TJ disruption,[36] causing barrier hyperpermeability, apoptotic cell death and astrocytosis.[37] Finally, it may lead to SAE.[3,36–38] We found that SNAI1 mediated TNF-α-induced hyperpermeability of brain microvessels and that DHA reversed the SNAI1 and OCLN level induced by TNF-α. In addition, SNAI1 overexpression mimicked the effect of TNF-α on OCLN, therefore, we inferred that DHA could reverse the effects of TNF-α on OCLN by decreasing SNAI1 expression. This may partially explain the mechanism by which artemisinins protect the BBB during sepsis.

Artemisinins decrease the expression of SNAI1 to reduce tumorigenesis and metastasis in cancer cells.[39,40] SNAI1 plays a role in many pathological processes. Notably, it regulates the endothelial-mesenchymal transformation in the vascular system.[41] Moreover, many studies have focused on SNAI1's role in barrier maintenance. SNAI1 was reported to repress the expression of TJs and/or AJs to mediate intestinal epithelial hyperpermeability.[42–45] By repressing the expression of vascular endothelial-cadherin (VE-cadherin) transcriptionally, SNAI1 participates in Mn-induced hyperpermeability of glomerular endothelial cells.[46] During acute lung injury, SNAI1 decreases the expression of TJs and AJs. Additionally, SNAI1 is involved in HMGB1-mediated pulmonary microvascular endothelial hyperpermeability.[47] Recent studies have reported that SNAI1 is related to BBB permeability. SNAI1 downregulates the expression of TJs (including OCLN) to mediate bacteria-stimulated brain endothelial hyperpermeability.[26,48] Here, we found that SNAI1 decreases the expression of OCLN to mediate TNF-α-induced BBB hyperpermeability. In addition, DHA reduces the expression of SNAI1 to decrease the permeability of BECs, suggesting that SNAI1 mediates the effects of artemisinins.

In conclusion, our study revealed that DHA protects against sepsis-induced BBB permeability and reversed TNF-α-induced OCLN expression by inhibiting SNAI1 expression. DHA could be used as a potential treatment for sepsis-induced brain damage.

4 | METHODS

4.1 | Mouse model

Male C57BL/6J mice (22-25 g) were obtained from Pengyue Experimental Animal Breeding. All the animals were housed at 21°C ± 1°C, with a relative humidity of 50% ± 1%, and a light/dark cycle of 12/12 h. All animal studies, including euthanasia, were performed in compliance with the regulations and guidelines of the Shandong First Medical University Institutional Animal Care Center.

Mice were randomly divided into three groups: the sham, CLP and CLP + DHA groups. CLP was performed as previously described, with minor modifications.[49] Briefly, the mice were anaesthetised with isoflurane. The abdomen was then sliced layer-by-layer with

longitudinal incisions (1.5-2 cm), and the cecum was isolated and exteriorized from the peritoneal cavity. The cecum was ligated at half the distance between the distal pole and the base. A 21G needle was used to puncture the cecal wall from one side to the other. Finally, the cecum was returned to the abdominal cavity and the abdomen was sutured. A total of 100 mg/kg DHA was used according to our previous study[50] and preliminary experiment. The sham group underwent the same operation without cecal ligation and puncture. One hour after CLP surgery, 100 mg/kg DHA (Sigma-Aldrich) was administrated by gavage to the mice, except for those in the sham group, which received the same amount of saline. After 24 h, mice brains and microvessels were collected for subsequent experiments.

4.2 | Isolation of mouse cerebral microvessels

Microvessel isolation was performed as previously described,[51] with minor modifications. The mice were killed, and the brains were removed. The brain meninges and meningeal vessels were then removed by rolling the tissues on dry paper. The cortices were isolated by removing the cerebellum, hippocampus and residual white matter. The samples were individually mixed in Dulbecco's phosphate buffered saline (DPBS) and homogenized in endothelial cell medium (ECM, Sciencell) at 2000 × *g* for 5 min at 4°C. Samples (pellets) were resuspended in 15% dextran-DPBS and centrifuged at 4°C, after which the supernatant was removed. DPBS was then used to wash the microvessel-containing pellet on a 40-μM cell strainer. Samples were then centrifuged again to obtain the final microvessel pellet, and either ice-cold protein lysis buffer or RNAiso Plus was used to obtain the protein or RNA of mouse cerebral microvessel, respectively.

4.3 | Cell culture

The hCMEC/D3 cells were cultured in ECM medium supplemented with endothelial cell growth factors (ECGS), 5% fetal bovine serum (FBS), and 1% penicillin-streptomycin. All cell culture flasks were precoated with type I rat tail collagen (Solarbio). Cells were seeded on collagen-coated flasks, cultured at 37°C in 5% CO_2 until 90% confluence, and then treated with 10 ng/mL TNF-α and/or DHA for 24 h. When cells were treated with TNF-α, the culture medium was replaced with ECM without growth factors or supplements (Lonza).

4.4 | Cell viability

hCMEC/D3 cells were seeded in a 96-well plate at a density of 5000 cells per well and incubated overnight. The cells were then treated with different concentrations of DHA and/or 10 ng/mL TNF-α. Cell viability was measured using a Cell Counting Kit-8 (CCK-8) (APExBIO). After treatment for 24 h, 10 μL CCK-8 reagent was added to the culture medium and samples were further incubated for 4 h at 37°C. Absorbance was read at 450 nm using a microplate reader (BioTek Epoch).

4.5 | Brain water content assay

Brain samples were dissected 24 h post-operation. As reported previously,[28] the brain water content was measured using the standard wet-dry method. The wet weights of the brain samples were quantified immediately after dissection. The dry weight was quantified after brain samples were dried in an oven at 100°C for 24 h. The brain water content was calculated using the following formula: (wet weight − dry weight)/wet weight × 100%.

4.6 | BBB permeability measurements in vivo

BBB permeability was determined using protocols modified from previous studies.[15] At 24 h post-operation, mice were anaesthetised and injected with Evans blue dye (2% in saline, 2 mL/kg) via the tail vein. One hour later, the mice were subjected to transcardial perfusion using 0.9% saline. Mouse brain tissue was separated and prepared for trichloroacetic acid (TCA) extraction according to a previously described protocol.[15] The amount of Evans blue dye was measured using the spectrophotometer at 620 nm. Evans blue albumin was used as a standard and the results was expressed as ng/mg of brain tissue.

4.7 | Evaluation of inflammatory cytokines TNF-α

The levels of TNF-α in the serum and cortex were determined 24 h post-operation; they were measured using commercially available mouse TNF-α ELISA kits (Elabscience). The assay was performed according to the manufacturer's instructions. Data were analysed using a microplate reader (BioTek Epoch).

4.8 | RT-qPCR

RT-qPCR was performed as described in our previous study.[52] Briefly, total RNA was extracted using RNAiso Plus (Takara Bio). A total of 1 μg RNA was reverse transcribed into complementary DNA (cDNA) by a 1st Strand cDNA Synthesis kit (Vazyme). RT-qPCR assay was performed using a SYBR qPCR Master Mix (Vazyme) in a CFX96 Real-Time System (Bio-Rad Laboratories). Mouse or human β-actin was used as an internal control. The sequences of the primers used are summarized in Table 1.

4.9 | Western blotting

Western blotting of mouse brain microvessel endothelial cells and hCMEC/D3 cells were performed as previously described.[52] The primary antibodies used rabbit anti-occludin (13409-1-AP, Proteintech), goat anti-SNAIL (ab53519, Abcam) and rabbit anti-GAPDH (14C10, Cell Signalling Technology). The horseradish peroxidase (HRP)-linked secondary antibodies were purchased from Proteintech.

TABLE 1 RT-qPCR Primer sequences

Gene	Sequence	Size (bp)	Tm (°C)
mSnai1			
Sense	TGTACCCGCCCAGAGCCTCC	122	60
Anti-sense	CCCCTGAGCGGGGTTCAAGC		
mOCLN			
Sense	GCTTATCTTGGGAGCCTGGACA	144	60
Anti-sense	GTCATTGCTTGGTGCATAATGATTG		
mβ-actin			
Sense	GGATGCAGAAGGAGATTACTGC	94	60
Anti-sense	CCACCGATCCACACAGAGTA		
hSNAI1			
Sense	GAGGCGGTGGCAGACTAG	178	60
Anti-sense	GACACATCGGTCAGACCAG		
hOCLN			
Sense	CCCCATCTGACTATGTGGAAAGA	78	60
Anti-sense	AAAACCGCTTGTCATTCACTTTG		
hβ-actin			
Sense	TTGCCGACAGGATGCAGAA	101	60
Anti-sense	GCCGATCCACACGGAGTACT		

Note: All sequences are in the 5′ to 3′ orientation.
Abbreviations: bp: base pair; Tm: temperature; Snai1: snail family transcriptional repressor 1; Ocln: occludin.

4.10 | IHC assay

IHC was performed as previously described.[52] Brain sections were incubated with rabbit anti-occludin antibody (13409-1-AP, Proteintech) overnight at 4°C, and then incubated with an anti-mouse/rabbit IHC kit (Maixin). Antigens were detected by DAB, and nuclear was detected by haematoxylin. The brain sections were photographed using an Olympus BX51 microscope (Olympus).

4.11 | IF assay

IF was performed according to a previous study.[52] Sections were incubated with the primary antibodies (rabbit anti-occludin (13409-1-AP, Proteintech) and goat anti-SNAI1 (AF3639, R&D)) in 4°C overnight. The next day, the sections were incubated with secondary antibodies (Alexa Fluor 488 goat anti-rabbit IgG) (ab150077, Abcam) and Alexa Fluor 488 donkey anti-goat IgG (ab150129, Abcam). The nucleus was stained with 4',6-diamidimo-2-phenylindole (DAPI). Images were photographed with a Leica DMi8 microscope.

4.12 | siRNA transfection

hCMEC/D3 cells were seeded in collagen-coated 6-well plates and grown to 70%-90% confluency. Human SNAI1 siRNA (Genepharma) were transiently transfected into hCMEC/D3 cells, and Lipofectamine RNAiMAX (Invitrogen) transfection reagent was used according to the manufacturer's protocol. The oligonucleotide sequences used were as follows:

NC-siRNA:
sense: 5′-UUCUCCGAACGUGUCACGUTT-3′;
antisense: 5′-ACGUGACACGUUCGGAGAATT-3′.
Human SNAI1 siRNA:
sense: 5′-CAGGACUCUAAUCCAGAGUTT-3′;
antisense: 5′-ACUCUGGAUUAGAGUCCUGTT-3′.

4.13 | Transfection of pCMV6-*SNAI1* plasmids

The hCMEC/D3 cells (1×10^5 cells per well) were plated on the collagen-coated 6-well plate and cultured to 60% confluence. Polyethylenimine (PEI, 25 kDa, Polysciences) 3 μg and 2 μg of pCMV6-*SNAI1* plasmids were added to each well. The transfection was performed as previously described.[53] After transfection for 24 h, the cells were pretreated with 100 ng/mL DHA for 1 h and then exposed to 10 ng/mL TNF-α for 24 h.

4.14 | FITC-dextran transwell assay

The hCMEC/D3 cells were seeded on the top of a collagen-coated 0.4 μM transwell insert (Corning Incorporated) and cultured to 95% confluence. Following pretreatment with DHA for 1 h, cells were exposed to TNF-α for 24 h, after which a FITC-dextran assay was performed.[52] First, 40 kDa FITC-dextran (10 mg/mL, Sigma-Aldrich) was

added to the upper chamber of the transwell system. After 6 h of exposure, the culture in the lower chamber was collected for fluorescence detection; an excitation wavelength of 485 nm and an emission wavelength of 520 nm were used.

4.15 | Statistical analysis

Data represents the mean values ± standard deviation (SD); they were calculated using GraphPad Prism program 5.0. The Student's unpaired 2-tailed *t* test was used for comparisons between two groups; the one-way ANOVA followed by post hoc LSD correction was used for comparisons of multiple groups. All statistics were performed with SPSS 22.0 (SPSS). Statistical significance was set at $P < .05$.

ACKNOWLEDGEMENTS

This study was supported by the National Nature Science Foundation of China (82171318, 81873473 and 91939110), Academic Promotion Program of Shandong First Medical University (2019QL014), Jinan City's Science and Technology Innovation Program of Clinical Medicine (202019175) and Shandong Taishan Scholarship (J.L.), Cultivation Fund for the First Affiliated Hospital of Shandong First Medical University QYPY2021NSFC0613. English language was edited by English speaking editors at Wiley Editing Services.

CONFLICT OF INTEREST

The authors declare that they have no known competing financial interests or personal relationships that could have appeared to influence the work reported in this paper.

DATA AVAILABILITY STATEMENT

The datasets used and/or analysed during the current study are available from the corresponding author on reasonable request.

ORCID

Ju Liu https://orcid.org/0000-0001-9932-2613

REFERENCES

1. Catarina AV, Branchini G, Bettoni L, De Oliveira JR, Nunes FB. Sepsis-associated encephalopathy: from pathophysiology to Progress in experimental studies. *Mol Neurobiol*. 2021;58(6):2770-2779.
2. Molnár L, Fülesdi B, Németh N, Molnár C. Sepsis-associated encephalopathy: a review of literature. *Neurol India*. 2018;66(2):352-361.
3. Danielski LG, Giustina AD, Badawy M, et al. Brain barrier breakdown as a cause and consequence of Neuroinflammation in sepsis. *Mol Neurobiol*. 2018;55(2):1045-1053.
4. Gu M, Mei XL, Zhao YN. Sepsis and cerebral dysfunction: BBB damage, Neuroinflammation, oxidative stress, apoptosis and autophagy as key mediators and the potential therapeutic approaches. *Neurotox Res*. 2021;39(2):489-503.
5. Abbott NJ, Patabendige AA, Dolman DE, Yusof SR, Begley DJ. Structure and function of the blood-brain barrier. *Neurobiol Dis*. 2010;37(1):13-25.
6. Lv J, Hu W, Yang Z, et al. Focusing on claudin-5: a promising candidate in the regulation of BBB to treat ischemic stroke. *Prog Neurobiol*. 2018;161:79-96.
7. Greene C, Campbell M. Tight junction modulation of the blood brain barrier: CNS delivery of small molecules. *Tissue Barriers*. 2016;4(1):e1138017.
8. Tu Y. Artemisinin—a gift from traditional Chinese medicine to the world (Nobel lecture). *Angew Chem Int Ed*. 2016;55:10210-10226.
9. Li D, Qi J, Wang J, et al. Protective effect of dihydroartemisinin in inhibiting senescence of myeloid-derived suppressor cells from lupus mice via Nrf2/HO-1 pathway. *Free Radic Biol Med*. 2019;143:260-274.
10. Dong F, Zhou X, Li C, et al. Dihydroartemisinin targets VEGFR2 via the NF-kappaB pathway in endothelial cells to inhibit angiogenesis. *Cancer Biol Ther*. 2014;15(11):1479-1488.
11. Crespo-Ortiz MP, Wei MQ. Antitumor activity of artemisinin and its derivatives: from a well-known antimalarial agent to a potential anticancer drug. *J Biomed Biotechnol*. 2012;2012:247597.
12. Kuang M, Cen Y, Qin R, et al. Artesunate attenuates pro-inflammatory cytokine release from macrophages by inhibiting TLR4-mediated Autophagic activation via the TRAF6-Beclin1-PI3KC3 pathway. *Cell Physiol Biochem*. 2018;47(2):475-488.
13. Zhang E, Wang J, Chen Q, Wang Z, Ju X. Artesunate ameliorates sepsis-induced acute lung injury by activating the mTOR/AKT/PI3K Axis. *Gene*. 2020;759:144969.
14. Souza MC, Paixao FH, Ferraris FK, Ribeiro I, Henriques M. Artesunate exerts a direct effect on endothelial cell activation and NF-kappaB translocation in a mechanism independent of plasmodium killing. *Malar Res Treat*. 2012;2012:679090.
15. Zuo S, Ge H, Li Q, et al. Artesunate protected blood-brain barrier via sphingosine 1 phosphate receptor 1/phosphatidylinositol 3 kinase pathway after subarachnoid hemorrhage in rats. *Mol Neurobiol*. 2017;54(2):1213-1228.
16. Feldman GJ, Mullin JM, Ryan MP. Occludin: structure, function and regulation. *Adv Drug Deliv Rev*. 2005;57(6):883-917.
17. Cummins PM. Occludin: one protein, many forms. *Mol Cell Biol*. 2012;32(2):242-250.
18. Furuse M, Itoh M, Hirase T, et al. Direct association of occludin with ZO-1 and its possible involvement in the localization of occludin at tight junctions. *J Cell Biol*. 1994;127(6 Pt 1):1617-1626.
19. Saito AC, Higashi T, Fukazawa Y, Otani T, Chiba H. Occludin and tricellulin facilitate formation of anastomosing tight-junction strand network to improve barrier function. *Mol Biol Cell*. 2021:mbc.E20-07-0464;32:722-738.
20. Erikson K, Tuominen H, Vakkala M, et al. Brain tight junction protein expression in sepsis in an autopsy series. *Crit Care*. 2020;24(1):385.
21. Nieto MA. The snail superfamily of zinc-finger transcription factors. *Nat Rev Mol Cell Biol*. 2002;3(3):155-166.
22. Hemavathy K, Ashraf SI, Ip YT. Snail/slug family of repressors: slowly going into the fast lane of development and cancer. *Gene*. 2000;257(1):1-12.
23. Arzumanyan A, Friedman T, Kotei E, Ng IO, Lian Z, Feitelson MA. Epigenetic repression of E-cadherin expression by hepatitis B virus x antigen in liver cancer. *Oncogene*. 2012;31(5):563-572.
24. Blanco MJ, Barrallo-Gimeno A, Acloque H, et al. Snail1a and Snail1b cooperate in the anterior migration of the axial mesendoderm in the zebrafish embryo. *Development*. 2007;134(22):4073-4081.
25. Peiro S, Escriva M, Puig I, et al. Snail1 transcriptional repressor binds to its own promoter and controls its expression. *Nucleic Acids Res*. 2006;34(7):2077-2084.
26. Kim BJ, Hancock BM, Bermudez A, et al. Bacterial induction of Snail1 contributes to blood-brain barrier disruption. *J Clin Invest*. 2015;125(6):2473-2483.
27. Ikenouchi J, Matsuda M, Furuse M, Tsukita S. Regulation of tight junctions during the epithelium-mesenchyme transition: direct repression of the gene expression of claudins/occludin by snail. *J Cell Sci*. 2003;116(Pt 10):1959-1967.
28. Zhao L, An R, Yang Y, et al. Melatonin alleviates brain injury in mice subjected to cecal ligation and puncture via attenuating inflammation,

apoptosis, and oxidative stress: the role of SIRT1 signaling. *J Pineal Res*. 2015;59(2):230-239.
29. Schwachtgen JL, Janel N, Barek L, et al. Ets transcription factors bind and transactivate the core promoter of the von Willebrand factor gene. *Oncogene*. 1997;15(25):3091-3102.
30. Zhang Y, Ding X, Miao C, Chen J. Propofol attenuated TNF-α-modulated occludin expression by inhibiting Hif-1α/ VEGF/ VEGFR-2/ ERK signaling pathway in hCMEC/D3 cells. *BMC Anesthesiol*. 2019;19(1):127.
31. Ahmed R, Poespoprodjo JR, Syafruddin D, et al. Efficacy and safety of intermittent preventive treatment and intermittent screening and treatment versus single screening and treatment with dihydroartemisinin-piperaquine for the control of malaria in pregnancy in Indonesia: a cluster-randomised, open-label, superiority trial. *Lancet Infect Dis*. 2019;19(9):973-987.
32. Kajubi R, Ochieng T, Kakuru A, et al. Monthly sulfadoxine-pyrimethamine versus dihydroartemisinin-piperaquine for intermittent preventive treatment of malaria in pregnancy: a double-blind, randomised, controlled, superiority trial. *Lancet*. 2019;393(10179):1428-1439.
33. Muhindo MK, Jagannathan P, Kakuru A, et al. Intermittent preventive treatment with dihydroartemisinin-piperaquine and risk of malaria following cessation in young Ugandan children: a double-blind, randomised, controlled trial. *Lancet Infect Dis*. 2019;19(9):962-972.
34. Shi Z, Chen Y, Lu C, et al. Resolving neuroinflammation, the therapeutic potential of the anti-malaria drug family of artemisinin. *Pharmacol Res*. 2018;136:172-180.
35. Wang Y, Wang Y, You F, Xue J. Novel use for old drugs: the emerging role of artemisinin and its derivatives in fibrosis. *Pharmacol Res*. 2020;157:104829.
36. Alexander JJ, Jacob A, Cunningham P, Hensley L, Quigg RJ. TNF is a key mediator of septic encephalopathy acting through its receptor, TNF receptor-1. *Neurochem Int*. 2008;52(3):447-456.
37. Semmler A, Hermann S, Mormann F, et al. Sepsis causes neuroinflammation and concomitant decrease of cerebral metabolism. *J Neuroinflammation*. 2008;5:38.
38. Kuperberg SJ, Wadgaonkar R. Sepsis-associated encephalopathy: the blood-brain barrier and the sphingolipid rheostat. *Front Immunol*. 2017;8:597.
39. Yu C, Sun P, Zhou Y, et al. Inhibition of AKT enhances the anti-cancer effects of Artemisinin in clear cell renal cell carcinoma. *Biomed Pharmacother*. 2019;118:109383.
40. Li Y, Zhou X, Liu J, et al. Dihydroartemisinin inhibits the tumorigenesis and metastasis of breast cancer via downregulating CIZ1 expression associated with TGF-beta1 signaling. *Life Sci*. 2020;248:117454.
41. Ke ZA, Cc B, Jh A, et al. Inhibitory effects of ursolic acid from Bushen Yijing formula on TGF-β1-induced human umbilical vein endothelial cell fibrosis via AKT/mTOR signaling and snail gene. *J Pharmacol Sci*. 2019;140(1):33-42.
42. Keshavarzian CBFYTMSLZA. Role of snail activation in alcohol-induced iNOS-mediated disruption of intestinal epithelial cell permeability. *Alcoholism Clinical & Experimental. Research*. 2011;35(9):1635-1643.
43. Liu W, Tao R, Ji X, Ran D, Xu X. The Gli1 lognail axis contributes to salmonella Typhimurium–.–nduced disruption of intercellular junctions of intestinal epithelial cells. *Cell Microbiol*. 2020;22(8):e13211.
44. Li YY, Xu QW, Xu PY, Li WM. MSC-derived exosomal miR-34a/c-5p and miR-29b-3p improve intestinal barrier function by targeting the snail/Claudins signaling pathway. *Life Sci*. 2020;257:118017.
45. Elamin E, Masclee A, Troost F, Dekker J, Jonkers D. Activation of the epithelial-to-mesenchymal transition factor snail mediates acetaldehyde-induced intestinal epithelial barrier disruption. *Alcohol Clin Exp Res*. 2014;38(2):344-353.
46. Gao P, Tian Y, Xie Q, Zhang L, Yan Y, Xu D. Manganese exposure induces permeability in renal glomerular endothelial cells via the Smad2/3-snail–VE-cadherin axis. *Toxicol Res*. 2020;5:5-692.
47. Luan Z, Bo H, Lei W, Jin S, Wang A. Unfractionated heparin alleviates human lung endothelial barrier dysfunction induced by high mobility group box 1 through regulation of P38–GSK3β–snail signaling pathway. *Cell Physiol Biochem*. 2018;46(5):1907-1918.
48. Yang R, Liu W, Miao L, et al. Induction of VEGFA and Snail-1 by meningitic Escherichia coli mediates disruption of the blood-brain barrier. *Oncotarget*. 2016;7(39):63839-63855.
49. Rittirsch D, Huber-Lang MS, Flierl MA, Ward PA. Immunodesign of experimental sepsis by cecal ligation and puncture. *Nat Protoc*. 2009;4(1):31-36.
50. Cheng Z, Qi R, Li L, et al. Dihydroartemisinin ameliorates sepsis-induced hyperpermeability of glomerular endothelium via up-regulation of occludin expression. *Biomed Pharmacother Biomed Pharmacother*. 2018;99:313-318.
51. Lee YK, Uchida H, Smith H, Ito A, Sanchez T. The isolation and molecular characterization of cerebral microvessels. *Nat Protoc*. 2019;14:3059-3081.
52. Liu F, Liu Q, Yuan F, et al. Erg mediates downregulation of claudin-5 in the brain endothelium of a murine experimental model of cerebral malaria. *FEBS Lett*. 2019;593(18):2585-2595.
53. Hsu CY, Uludag H. A simple and rapid nonviral approach to efficiently transfect primary tissue-derived cells using polyethylenimine. *Nat Protoc*. 2012;7(5):935-945.

SUPPORTING INFORMATION

Additional supporting information can be found online in the Supporting Information section at the end of this article.

How to cite this article: Liu F, Liu J, Xiang H, et al. Dihydroartemisinin protects blood–brain barrier permeability during sepsis by inhibiting the transcription factor SNAI1. *Clin Exp Pharmacol Physiol*. 2022;49(9):979-987. doi:10.1111/1440-1681.13683